Geographic Location Estimation from ENF Signals with High Accuracy

Huancheng Zhou, Hongyi Duanmu, Jiacheng Li, Yike Ma, Jun Shi, Zhihao Tan, Xiaohan Wang, Liuyu Xiang, Heqin Yin, Weihai Li*

Abstract—The Electric Network Signals (ENF) is the frequency characteristic of power distribution system, and can be captured in the form of power or audio recordings supplied by corresponding power system. The multi-dimensional diversity of the ENF between different regions allows it become a criterion of geographic localization. This triggered a lot of research on forensic authentication of digital and audio recordings. In this paper, we present a ENF-based location estimation system that integrates extraction and classification of power and audio signals from power grids. We uses several methods including autoregressive model and wavelet analysis to extract the statistical diversity of ENF signals as a whole to investigate the region-of-recording. The data is then classified by Support Vector Machine (SVM). We also built local sensing circuit to measure the local power grid data, and compare with the training data. The proposed scheme not only inherits high accuracy for power recordings, but also achieves improvements in audio recordings by pre-processing and utilization of higher harmonics. Extensive analytical and experimental results are presented which shows the accuracy and flexibility of our proposed system. We achieve accuracy rate of 93.3% for power signals and 80% for audio signals.

Index Terms—Electric network frequency, location estimation, machine learning, sensing circuit

◆

1 INTRODUCTION

THE Electric Network Frequency(ENF) analysis has become a promising tool for region-of-recording authentication and forgery detection in multimedia recordings including audio and video. The ENF signal reflects the supply frequency of electric power in distribution networks of a power grid, commonly with a mean value of 60Hz in the United States or 50Hz in most other parts of the world. The vibrations of ENF therefore contains time-varying and location-sensitive information of the original audio/video/power recordings, and are used for media time-stamping [1] and region-of-recording identification [2]. To capture the local ENF signals, we can extract from power recordings measured using a signal recorder, or multimedia recordings carrying background noise generated by mains-powered electronic devices like battery-powered device [3]. Some researches finds that ENF can also be captured by indoor lighting using optical sensors and video cameras [4].

In this paper, we report how we extract ENF signals from power and audio recordings, and how we apply the state-of-arts machine learning methods for location clas-

sification. We expand our research for audio recordings and power recordings separately. For power recordings, we adopt several commonly used methods to extract ENF signal, such as spectrograms in time/frequency domain, short-time Fourier Transformation in frequency domain, zero-crossing rate in time domain [5], and autoregressive model. For audio recordings, we consider combining weighted spectrum [6], and adopt the spectral subtraction [7] method to pre-process audio recordings. Furthermore, observations during ENF extractions are given for building up an effective classifier. One novel improvements come from the utilization of higher harmonics apart from spectral band surrounding the mean value. To represent the fluctuations in a quantitative manner, we choose several features both from original recording and ENF signal. Then we build a classifier using the one-vs-all implementation of support vector machine to process the input of features that can represent characteristics of a power grid region. We also build up a sensing circuit used for local recordings to compare with other training data to prove the effectiveness and robustness of our design.

The rest of this paper is organized as follows. Section II describes how we pre-process the recordings and perform extraction for various features from power and audio recordings, with our observations of how ENF signals fluctuate in different regions and in different frequency bands. In Section III, we then explains our implementations on one-vs-all model by Support Vector Machine (SVM) and gives a scope of the classification system, with the results of practice data, test data and local data to show the accuracy and flexibility of our system. Section IV illustrates the design and the actual picture of our sensing circuit used for local recordings, with common problems and our countermeasures, and we gives the comparisons with other training data. Finally Section V concludes our work.

- *Huancheng Zhou, Jiacheng Li, Jun Shi and Heqin Yin are with the Department of Information Security, School of Information Science and Technology, University of Science and Technology of China.*
  E-mail: {zhouhc,colastar,shi1995,yhq123}@mail.ustc.edu.cn
- *Hongyi Duanmu, Xiaohan Wang and Liuyu Xiang are with the Department of Electronic Engineering and Information Science, School of Information Science and Technology, University of Science and Technology of China.*
  E-mail: {darksnip,wxh1996,wuhanxly}@mail.ustc.edu.cn
- *Yike Ma, Zhihao Tan are with the Department of Information Security, School of Information Science and Technology, and School of the Gifted Young, University of Science and Technology of China*
  E-mail: {domi, tzh0799}@mail.ustc.edu.cn
- ** Weihai Li is the supervisor of the team, with the Department of Electronic Engineering and Information Science and the Department of Information Security, School of Information Science and Technology.*
  E-mail: whli@ustc.edu.cn

2 EXTRACTION

The extraction of ENF signals acts as the fundamental of accurate and effective location-based classification system. Targeting at the chaotic nature of audio recordings, several pre-processing mechanisms are exercised to reduce the noise. Then an initial extraction is performed for ENF signals among spectral bands near mean-value and higher harmonics by detailed algorithm based on autoregressive model and fast Fourier transformation. Feature extraction acts as the concluding extraction, which is made by statistical mechanisms in various domains including wavelet domain to provide 36 characteristics as input to classifier.

2.1 Pre-processing

2.1.1 Incentives for Audio Recordings

If without any pre-processing, the frequency vibrations of audio recordings is irregular. This is because our algorithm extracts the frequency with highest weight, while the frequency distribution of audio signals is self-evidently chaotic. As a result, pre-processing is demanded before further extraction from audio recordings is carried out. By observation of training data, it is discovered in the Figure 1 that apart from the original frequency, there are clear and fine line around the higher harmonic in the frequency distribution graph. And these higher harmonics appear to be clear and similar with each other.

(a) Frequency pattern of Area A   (b) Frequency distribution
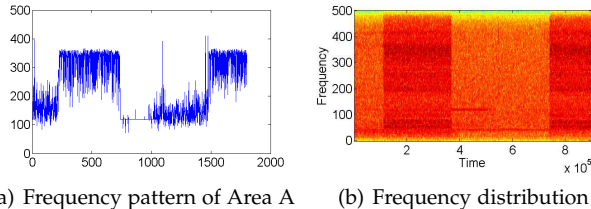
Fig. 1. ENF graph and frequency distribution of audio signals without pre-processing

The philosophy of pre-processing is to de-noise the input signals and enhance traces of the ENF signals in various spectral bands from the original audio recordings.

2.1.2 Spectral Subtraction

To purify the audio signal data, we take the idea of spectral subtraction [7], one of the speech enhancement algorithms, to de-noise the audio recordings. Results of spectral subtraction on audio recordings are shown in Figure 2.

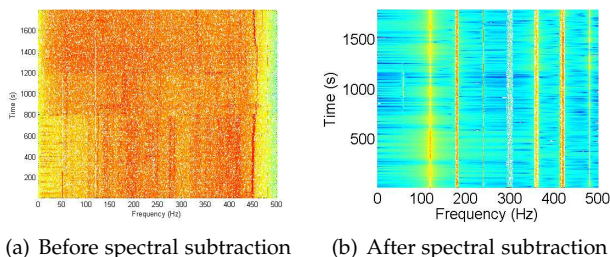(a) Before spectral subtraction   (b) After spectral subtraction

Fig. 2. Typical spectrogram of original audio recording and audio recording after de-noising by spectral subtraction

The spectral subtraction starts as followed. Firstly, we expand the audio signals in the short-time Fourier domain:

$$\mathcal{X}(\omega, n) = S(\omega, n) + I(\omega, n)$$

The $\mathcal{X}(\omega, n)$ represents the original audio recordings, regarded as a mixture of clean signal and interference. Then $S(\omega, n)$ and $I(\omega, n)$ represent the clean signal and interference signal respectively. By subtracting the background noise $I(\omega, n)$, we can reach a approximatively good estimation of the clean signal containing ENF information. As estimating $I(\omega, n)$ could be hard, we turn to subtract a certain percentage of the maximum value of $\mathcal{X}(\omega, n)$, as a constant-level prediction of interference. This is because the maximum value usually goes upstairs to several orders of magnitude, far larger than the mean value of $\mathcal{X}(\omega, n)$. Finally, we obtain the time-domain signal by inverse Fourier transformation of the subtracted magnitude spectrum using the phase of $\mathcal{X}(\omega, n)$.

Remark 1. De-noising on audio recording fails to recover the ENF of some regions with great interference, which requires us to turn to higher harmonics instead. Observations shows that almost all audio recordings fortunately have at least one clear spectral band that are not seriously interfered. Such intact spectral bands of audio recordings are accepted in our pre-processing phase and used for training later. However, as the interference appears random, selecting fine bands is difficult for a machine to achieve without proper algorithms and experimental testing. Due to the limitation of time, we have done the selecting job manually. The selected results have been attached in our submitting materials. Please be aware of this when reproducing the results.

2.1.3 Impulse Elimination

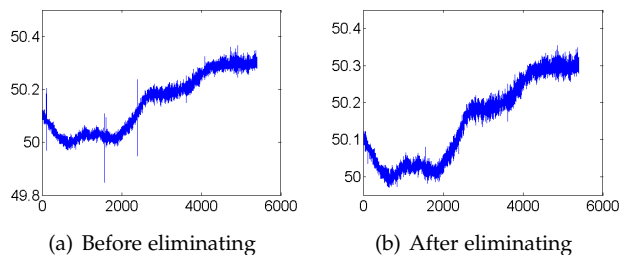

(a) Before eliminating   (b) After eliminating

Fig. 3. ENF signal before and after eliminating the impulse

ENF signals are sensitive to slight changing in power grid, and impulses may appear due to some distortions in the original data. By extensive experiments, we find that this may interfere our estimation of the several features of ENF signal, such as the mean value and the range. We eliminate such impulses by the following ways:

- Find a referencing mean value x_{avg} within a region.
- Estimate the distribution of points $x(n)$ in ENF signals by the distance away from x_{avg}.
- Fix the apparently low-frequency value by the mean value x_{avg} to replace the sudden value $Pr[x(k)] \ll 1$.

The elimination shows novel improvements in estimating mean value and fluctuations of the ENF signals, without

affecting the majority of input data. The results are shown in figure 3.

Remark 2. When extracting ENF signal from audio recordings, we finds the ENF signals could be extracted from more discovered that such ENF can be extracted from more than the higher harmonics, like some 'shifting' harmonics.

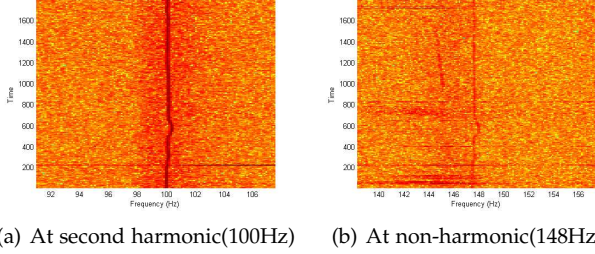(a) At second harmonic(100Hz)   (b) At non-harmonic(148Hz)

Fig. 4. Shifting phenomenon in non-harmonic area by ENF fluctuations observations

As it can be seen in Figure 11, these lines appeared shifted from the harmonics, and containing the ENF signal since their fluctuations resemble ENF signals around mean. The extraction of these lines are beyond the scope of our discussion, and will be included in our future work.

2.2 Initial Extraction

2.2.1 Algorithm for Frequency

The extraction of our estimation system focuses on geographically related differences of ENF signals. Practical data shows human-readable and evident distinctions on the mean value and fluctuations of waveforms. In our estimation system, we use autoregressive model, hamming windows and fast Fourier transform to extract the ENF signals as an intial step as followed.

- Input signal is a discrete digital signal $x(n)$.
- Calculate the Autoregressive (AR) function of $x(n)$, i.e. the first difference.

$$x'(n) = x(n) - x(n-1)$$

- Prior to fast Fourier transform, use Hamming windows $h(n)$ to the signals $x(n)$ and the first difference $x'(n)$ to reduce spectrum leakage.

$$x_1(n) = x(n)h(n), \ x_1'(n) = x'(n)h(n)$$

- Calculate the N-points fast Fourier transform of $x_1(n)$ and $x_1'(n)$.

$$\mathcal{X}(K) = \mathcal{FFT}(x_1(n)), \ \mathcal{X}'(K) = \mathcal{FFT}(x_1'(n))$$

- Find the maximum module of $\mathcal{X}(K)$ and $\mathcal{X}'(K)$.

$$|\mathcal{X}(K_{max})|>|\mathcal{X}(K_{other})|, \ |\mathcal{X}'(K_{max})|>|\mathcal{X}'(K_{other})|$$

- Calculate the decimation factor f_a.

$$f_a = \frac{\pi K_{max}}{N \sin(\pi K_{max}/N)}$$

- Calculate the frequency f_r with the sampling frequency f_m.

$$f_r = \frac{f_m f_a |\mathcal{X}'(K_{max})|}{2\pi |\mathcal{X}(K_{max})|}$$

This algorithm extracts the frequency components with highest weight in distinct waves. By separating the input data continuously into a series of groups, we calculate the frequency f_r for each group and investigate its vibrations in a long period, called the ENF signals. Figure 5 shows ENF signals extracted from the training data. The ENF between some regions shows human-readable and evident difference, though some are similar(e.g. Area A and Area E). For such regions, other accurate and subtle characteristics is demanded to distinguish them.

2.2.2 Utilization of Higher Harmonics

ENF signals can not only be found around mean value, but also higher harmonics areas. Figure 6 shows results of ENF signal at each harmonic level adjusted into the same scale. The ENF signals extracted from different spectral bands appear to be clear and fine lines and they coincide with each other.

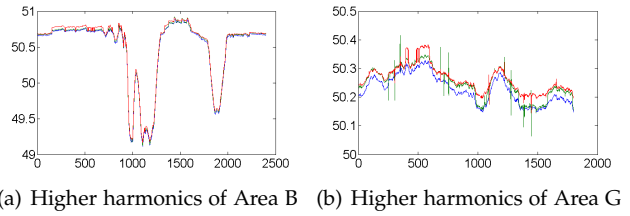(a) Higher harmonics of Area B   (b) Higher harmonics of Area G

Fig. 6. Similarity of higher harmonics extracted from different spectral bands in ENF signals

Retrospect the audio recordings, and we notice the original ENF signal near mean value is interfered by noise. Extracting ENF signal directly from the original data without pre-processing phase result in distorted waveform. However, by effective pre-processing including spectral subtraction and impulse elimination, the ENF waveform can be obtained around useful and remarkable high harmonics and enable the method of spectral combining which is mentioned in [6]. By pre-processing and higher harmonics utilizing, we make the audio recordings look more 'like power' to better represent characteristics of a region.

2.3 Feature Extraction

After pre-processing and initial extraction, the original recordings have been de-noised and sufficient ENF signal details are collected. To offer accurate and subtle characteristics of such data, we implements parameters of the autoregressive model, statistical values of ENF signals, statistical values of wavelet transform, energy percentage of wavelet transform. In total, we adopt 36 features that are extracted from both the ENF signal and the original recording.

2.3.1 Autoregressive Model

Autoregressive (AR) model are widely used in statistics and signal processing to represent the random process and reveal the time-varying linear properties. [2], [8], [9] have used autoregressive model as a manner to analyse the ENF signals. We model the ENF segment $s[n]$ as followed.
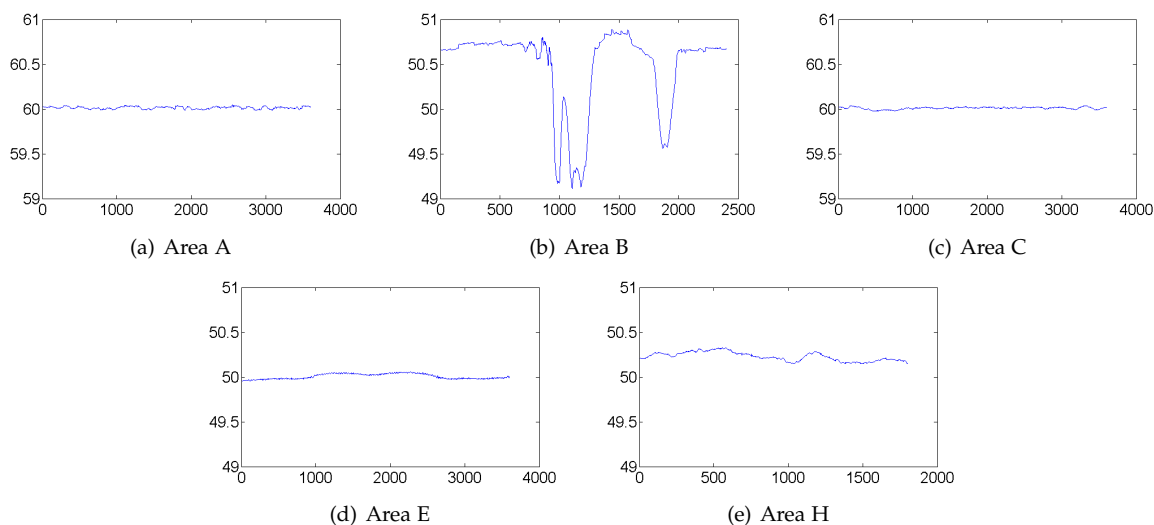
$$s[n] = a_1 s[n-1] + a_2 s[n-2] + v[n]$$

(a) Area A   (b) Area B   (c) Area C

(d) Area E   (e) Area H

Fig. 5. ENF graphs extracted from the training data

We adopt the two AR parameters a_1 and a_2, and the variance of the signal $v[n]$. The first two of them will represent the autoregressive model while the third describes how well the ENF signal fits in this model.

2.3.2 Wavelet Analysis

Wavelet analysis is a tool with purposefully properties for signal processing. We consider a wavelet decomposition of 9 levels, then acquire the variance of a_9, d_1 d_9. We call the a_9 as the approximation coefficient and d_1-d_9 as the detail coefficients. The wavelet decomposition structure is shown in Figure 7.
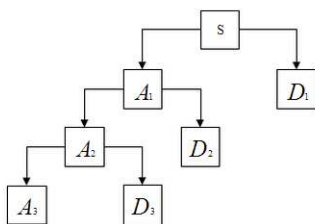

Fig. 7. Wavelet decomposition structure

Additionally, we take the variance of the reconstructed signals at each level because of the property that noise is reduced during wavelet reconstruction.

2.3.3 Energy Coefficients

Wavelet analysis can also provide evidence on industrialization level, which is related to geographic location. Regarding the fact that more high-power users exist in the power system, the steadier the power system is, and the approximation power coefficients will better describe the region. On the other hand, detail energy coefficients reflects the factory with more low-power users. As the ratio of power of different frequency bands varies as the industrialization level from region to region, we adopt the energy coefficients from wavelet decomposition to represent the ratio of power in different spectral bands. The energy coefficients from region A and I are listed in Table 1.

TABLE 1
Energy coefficients from different regions from wavelet spectrum

	I_A2	A_P9
a9	0.00468	0.006475
d1	29.72075	3.554942
d2	29.46764	13.12661
d3	25.71437	39.03955
d4	12.80335	44.09225
d5	1.618713	0.00925
d6	0.457584	0.015125
d7	0.147098	0.038401
d8	0.057055	0.088295
d9	0.008763	0.029104

2.3.4 Summary of Features

TABLE 2
All of the extracted 36 features that can represent characteristics included in the classification system

Index	Feature
1	$\text{var}(a_9)$
2-10	$\text{var}(d_1)$-$\text{var}(d_9)$
11	var(approximation after 9-level wavelet analysis from a_9)
12-20	var(signal reconstructed from d_1 and d_9)
21	a_9 energy-percentage
22-30	d_1-d_9 energy-percentage
31-32	linear prediction coefficient of autoregressive (AR)
33	least mean square deviation of autoregressive (AR)
34	mean(signal)
35	var(signal)
36	var(range(signal))

3   CLASSIFICATION

Classification will distinguish different power grid recordings into different region-of-recording. The classifier will learn a variety of characteristics from training data during the training phase, then exercise on practice data and test data to show the results. In this section, we explain our design for the geographic location classification system, show and discuss the classification results obtained on the practice data. Our classifier follows a design of multi-class classifier in a one-vs-all manner, based on the Support Vector Machine (SVM) algorithm. Experimental results on practice data and test data are given to prove the accuracy of our system. We achieve accuracy rate of 93.3% for power signals and 80% for audio signals.
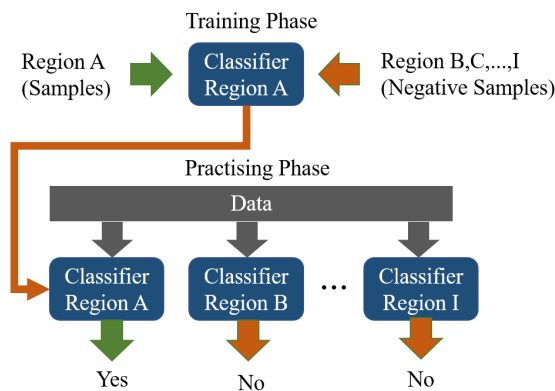

Fig. 8. Training phase and practising phase of our one-vs-all multi-class classifier

3.1   Design

3.1.1   Supervised Learning

For the classification with support of unknown class, we implements the **one-vs-all** classification method, which uses the following approach: regarding the first class as samples and the rest as negative samples, we get a classifier through SVM training algorithm that could identify whether data belongs to the first category. Then, we do the same to the next class until all the known classes are processed. By sending the input data to all these classifiers, we can get the feedback of the classifiers to know how well the test data belongs to a particular class. If only one class matches, we assume that the data belongs to this class with high assurance. Otherwise, if the data odes not belong to any particular class or belongs to more than one particular class, we assume the data belongs to an unknown class.

In our implementation, we uses Least Squares Support Vector Machines (LSSVM) library, which includes a multi-class SVM system that integrates one-vs-all method. Depending on the specified task of the competition, we need to train nine SVM classifiers to identify whether the practising data belongs to a particular class. The nine classifiers constitutes our geographic location estimation system.

3.1.2   Training

This study selects a total of 9 gird data from difference regions from training data, includes both the power recordings and audio recordings. We first divide each data into small data of three minutes, then extract the feature vectors from these small data. All the feature vectors are marked with the corresponding region information for supervised learning. After all feature vector data is accepted by the training algorithm, the classification system is built. Then, we input the feature vector data extracted from the practising data into the classification system and obtain each result of the test data. We use the results of small data to assign votes to each possible class. The final winning class is the class with the largest number of votes receiving from all the small data slices.

3.2   Results

3.2.1   Practising Data

Table 3 shows the estimating accuracy of the power recordings. We notice that one data extracted from Region C was classified to Region G, which results from the features similarity. Still, the result shows the feasibility of the SVM classifier. The amount of audio data is not large enough to justify the accuracy of classification. But since the audio signal shares more noise in the extraction phase, it is expected the audio recordings result in less accuracy.

TABLE 3
Power-Recording-Only Practising Data Matching Accuracy of
Presented Estimation System

Region	Accuracy(%)
A	100
B	100
C	95
D	100
E	100
F	100
G	100
H	100
I	100

The test result of practising data is given as followed and the accuracy is 88%. In details, 93.3% for power recordings, and 80% for audio recordings.

```
AHCFF,BGIND,AFBDI,INBAE,HBBAD,
AGHGB,DDCHG,EAGHI,EHECF,FNGNI
```

3.2.2   Test Data

We hereby submit the following results of the test dataset using our classification system to the Committee.

```
NDDCD,HHDAF,AAGBG,BFCEH,
GHHHG,HFDAI,DNFII,CECBD,
EAIBE,FGNAG,CINIG,HAEFC,
CNFDG,CECGI,EICEA,BEBHA,
DIHNG,AABIH,ANDBA,GBFBB
```

3.2.3   Local Data

In our implementation, we collect the power grid recordings of **Hefei City**, and analyse the similarity of Hefei recordings with the given regions A-I. Results show that Hefei City belongs to no area of Region A-I.

Fig. 9. The scope of sensing circuit

We compare the Hefei recordings as followed: starting from a SVM classifier, the SVM classifier is similar to getting a linear relationship in the high-dimensional space. For each test vector, it is regarded as a sample point of the high dimension space. By using each of the nine classifiers to calculate the distance, and mapping the normalized distance to 0-100%, we make a percentage of the similarity, which is shown in Table 4. The table shows that data in Hefei with B,C,H three regions have a little number of high similarity, but the similarity with Region A is substantially zero.

TABLE 4
Similarity of Hefei area and other input regions

Region	Similarity(%)
A	0.4301
B	23.9524
C	26.7552
D	13.4997
E	9.3941
F	13.4251
G	6.3634
H	23.3694
I	17.7172

4 SENSING CIRCUIT

The region-of-recording begins on capturing the power grid signals with high quality. By using fundamental electronic engineering devices, we construct a measurement system that automatically record and save long-period electricity data. The actual picture of our device is shown in Figure 9. Circuit diagram of our sensing circuit is shown in Figure 10.
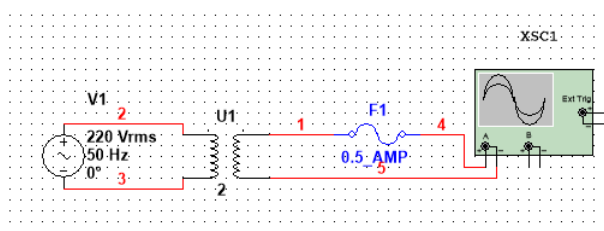

Fig. 10. Circuit diagram of our sensing circuit

In order to measure the power signal in the socket, we use the transformer to lower the voltage. Then we connect it to the oscilloscope to record the waveform data. We save data for more than every an hour, and get a total of ten data measured at different times in ten days. The following figure shows the original waveform of idle time and peak time based on the electricity consumption. It shows that the peak time waveform is unstable, reflecting the large varying range of the power signal. However, during some other time, such as 2 or 6 o'clock pm in China, the ENF measured is relatively stable, meaning the little time-varying range of the power signal.
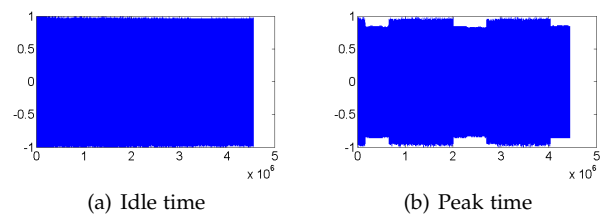

(a) Idle time   (b) Peak time

Fig. 11. Original waveform on different electricity consumption time

Remark 3. Specified data processing should be made after collection. We find that our original data has a remarkably strong energy distribution around 0Hz compared with the training data(power recordings). We decide to use a high pass filter to eliminate its effect, as is shown in Figure 12.
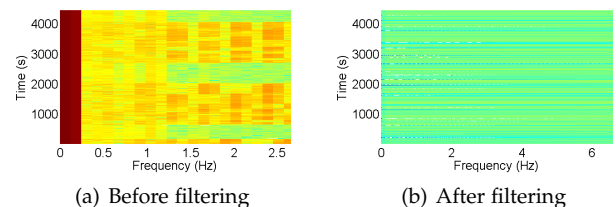

(a) Before filtering   (b) After filtering

Fig. 12. Circuit measurement results before and after high pass filter

5 FUTURE WORK

Due to the time limitation and knowledge restriction, there are space to improve the accuracy of the proposed system, which we regard as the future work. For spectral subtraction, we use a constant-level approximation to represent the noise in short-time Fourier domain. By further studying of fluctuations, higher-order approximation of noise signal could be made and fine-grained de-noising working on a less time-varying range could improve the de-noising.

For impulse elimination, mathematical proof of the optimal properties can be deeper researched and such mechanics might be expanded into more researches in this field. For higher harmonics, we discover the similarity of such signals, while electronic explanations are not sufficiently given, and accurate and automatic detection and evaluation of fine spectral bands should be developed. The feature selections adopted in our projects should also be examined by scientific method like backward greedy feature selection, while this is a time-consuming challenge due to the number of features.

6 CONCLUSIONS

In this paper, a variety of methods are adopted in sensing, extracting, classifying the ENF signal to estimate and predict the geographic location. By using higher harmonics and denoising techniques, we construct a region-of-recording estimation system with high accuracy from audio and power recordings. Experimental results show that our proposed system satisfies the requirements of the competition with accuracy and flexibility.

REFERENCES

[1] R. Garg, A. Varna, and M. Wu, "Modeling and analysis of electric network frequency signal for timestamp verification," in *Information Forensics and Security (WIFS), 2012 IEEE International Workshop on*, Dec 2012, pp. 67–72.

[2] A. Hajj-Ahmad, R. Garg, and M. Wu, "Enf-based region-of-recording identification for media signals," *Information Forensics and Security, IEEE Transactions on*, vol. 10, no. 6, pp. 1125–1136, June 2015.

[3] N. Fechner and M. Kirchner, "The humming hum: Background noise as a carrier of enf artifacts in mobile device audio recordings," in *IT Security Incident Management IT Forensics (IMF), 2014 Eighth International Conference on*, May 2014, pp. 3–13.

[4] R. Garg, A. Varna, A. Hajj-Ahmad, and M. Wu, "Seeing enf: Power-signature-based timestamp for digital multimedia via optical sensing and signal processing," *Information Forensics and Security, IEEE Transactions on*, vol. 8, no. 9, pp. 1417–1432, Sept 2013.

[5] C. Grigoras, "Applications of enf criterion in forensic audio, video, computer and telecommunication analysis," *Forensic Science International*, vol. 167, no. 23, pp. 136 – 145, 2007, selected Articles of the 4th European Academy of Forensic Science Conference (EAFS2006) June 13-16, 2006 Helsinki, Finland.

[6] A. Hajj-Ahmad, R. Garg, and M. Wu, "Spectrum combining for enf signal estimation," *Signal Processing Letters, IEEE*, vol. 20, no. 9, pp. 885–888, Sept 2013.

[7] S. Boll, "Suppression of acoustic noise in speech using spectral subtraction," *Acoustics, Speech and Signal Processing, IEEE Transactions on*, vol. 27, no. 2, pp. 113–120, Apr 1979.

[8] C. Grigoras, "Applications of enf analysis in forensic authentication of digital audio and video recordings," *J. Audio Eng. Soc*, vol. 57, no. 9, pp. 643–661, 2009.

[9] M. Wu, "Enf: Power signature for information forenscis," http://www.mast.umd.edu/index.php/enf-menu.

Huancheng Zhou Huancheng Zhou is working toward the bachelor's degree from University of Science and Technology of China. He has been with the School of Information Science and Technology since 2013. His research interests include wavelet analysis theory.

Jiacheng Li Jiacheng Li is working toward the bachelor's degree from University of Science and Technology of China. He has been with the Department of Information Security, School of Information Science and Technology since 2013, and the talent program in computer and information science and technology since 2013. In 2015, he was a teaching assistant with School of Information Science and Technology. His research interests include applied cryptography.
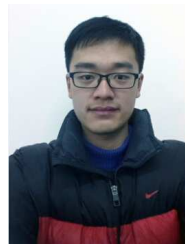
Liuyu Xiang Liuyu Xiang is working toward the bachelor's degree from University of Science and Technology of China. He has been with the Department of Electronic Engineering and Information Science, School of Information Science and Technology, and the talent program in computer and information science and technology since 2014. His research interests include speech enhancement.
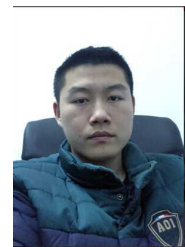
Heqin Yin Heqin Yin is working toward the bachelor's degree from University of Science and Technology of China. He has been with the Department of Information Security, School of Information Science and Technology since 2013. His research interests include Software Defined Network (SDN).

Yike Ma Yike Ma is working toward the bachelor's degree from University of Science and Technology of China. She has been with the Department of Information Security, School of Information Science and Technology, and School of the Gifted Young since 2013. Her research interests include music technology and information security.

Xiaohan Wang Xiaohan Wang is working toward the bachelor's degree from University of Science and Technology of China. He has been with the Department of Information Security, School of Information Science and Technology since 2013. His research interests include computer vision and machine learning.

Jun Shi Jun Shi is working toward the bachelor's degree from University of Science and Technology of China. He has been with the Department of Information Security, School of Information Science and Technology since 2013. His research interests include smart grids.

Hongyi Duanmu Hongyi Duanmu is working toward the bachelor's degree from University of Science and Technology of China. He has been with the Department of Electronic Engineering and Information Science, School of Information Science and Technology since 2013, and the talent program in computer and information science and technology since 2013. His research interests include speech recognition.

Zhihao Tan Zhihao Tan is working toward the bachelor's degree from University of Science and Technology of China. He has been with the Department of Information Security, School of Information Science and Technology, and School of the Gifted Young since 2013. His research interests include network security protocols.